

VUV photoionization of the CH2NC radical adiabatic ionization energy and cationic vibrational mode wavenumber determinations

Bérenger Gans, Sebastian Hartweg, Gustavo A Garcia, Séverine Boyé-Péronne, Oliver J Harper, Jean-Claude Guillemin, Jean-Christophe Loison

▶ **To cite this version:**

Bérenger Gans, Sebastian Hartweg, Gustavo A Garcia, Séverine Boyé-Péronne, Oliver J Harper, et al.. VUV photoionization of the CH2NC radical adiabatic ionization energy and cationic vibrational mode wavenumber determinations. Physical Chemistry Chemical Physics, 2020, 22 (22), pp.12496-12501. 10.1039/d0cp01901a . hal-02862237

HAL Id: hal-02862237

https://univ-rennes.hal.science/hal-02862237

Submitted on 11 Jun 2020

HAL is a multi-disciplinary open access archive for the deposit and dissemination of scientific research documents, whether they are published or not. The documents may come from teaching and research institutions in France or abroad, or from public or private research centers.

L'archive ouverte pluridisciplinaire **HAL**, est destinée au dépôt et à la diffusion de documents scientifiques de niveau recherche, publiés ou non, émanant des établissements d'enseignement et de recherche français ou étrangers, des laboratoires publics ou privés.

PCCP

ARTICLE TYPE

Cite this: DOI: 00.0000/xxxxxxxxxx

VUV photoionization of the CH_2NC radical: adiabatic ionization energy and cationic vibrational mode wavenumber determinations

Bérenger Gans,*[a] Sébastian Hartweg,[b] Gustavo A. Garcia,[b] Séverine Boyé-Péronne,[a] Oliver J. Harper,[a] Jean-Claude Guillemin,[c] and Jean-Christophe Loison*[d]

Received Date
Accepted Date

DOI: 00.0000/xxxxxxxxxx

The photoelectron spectroscopy of CH_2NC (isocyanomethyl) radical species is investigated for the first time between 9.3 and 11.2 eV in the vicinity of the first photoionizing transition $X^+\,^1A_1 \leftarrow X\,^2B_1$. The experiment combines a microwave discharge flow-tube reactor to produce the radicals through the $CH_3NC + F \rightarrow CH_2NC + HF$ reaction, a VUV synchrotron radiation excitation, and a double imaging electron/ion coincidence spectrometer which allows the recording of mass-selected threshold photoelectron spectra. Assignment of the observed vibrational structure of CH_2NC^+ cation is guided by *ab initio* calculations and Franck-Condon simulations. From the experimental spectrum, the first adiabatic ionization energy of the CH_2NC radical is measured at 9.439(6) eV. Fundamental wavenumbers are determined for several vibrational modes of the cation: $\tilde{\nu}_1^+$(CH_2 symmetric stretch) = 2999(80) cm^{-1}, $\tilde{\nu}_2^+$(N–C stretch) = 1925(40) cm^{-1}, $\tilde{\nu}_4^+$(H_2C–N stretch) = 1193(40) cm^{-1}, $\tilde{\nu}_6^+$(CNC out-of-plane bend) = 237(50) cm^{-1}, and $\tilde{\nu}_8^+$(CH_2 rock) = 1185(60) cm^{-1}.

1 Introduction

Isocyanides (or isonitriles, R-NC), isomers of the most stable cyanide compounds (or nitriles, R-CN), are important species in interstellar media and planetary atmospheres because their formation pathways strongly constrain the photochemical models of these media. The most abundant isocyanide compound is the hydrogen isocyanide (HNC) which is ubiquitous in the interstellar medium,[1] and present in comets[2] and in Titan's atmosphere.[3] In many objects, such as comets, the mechanism of formation of isocyanide is still unclear. Among the simplest isocyanides, HCNC and CH_2NC are expected to be present in dense molecular clouds, although not detected yet. Indeed, their precursor CH_3NC has been observed in the Horsehead Photon-Dominated Region[4] and in solar-type protostars.[5] Using their known spectral signatures, larger similar molecules such as HNCCC and HCCNC have been detected in dense molecular clouds such as TMC-1[6] and L1544.[7] Very recently, CNCN and $C_2N_2H^+$ have also been detected,[8–10] highlighting the importance of ionic chemistry in understanding the isonitrile formations and their role in astrochemistry. Indeed, CH_2NC is expected to be produced through the electronic dissociative recombination of the CH_3CN^+ and CH_2CNH^+ cations since the transition state of the $CH_2CN \rightarrow CH_2NC$ isomerization path is located only +209 kJ/mol above the CH_2CN ground state calculated at M06-2X/AVTZ using Gaussian16.[11] This barrier is well below the exothermicities of the $CH_3CN^+ + e^- \rightarrow CH_2CN + H$ and $CH_2CNH^+ + e^- \rightarrow CH_2CN + H$ reactions (−771 kJ/mol and −552 kJ/mol, respectively, calculated at M06-2X/AVTZ using Gaussian16[11]), in good agreement with the value calculated by Moran *et al.* (+214 kJ/mol calculated at the MP4/6-311++G level).[12] In addition, CH_2NC is expected to be one of the main products of the CN + CH_2CO reaction.[13,14] In this context, the study of the vacuum ultraviolet (VUV) photoionization spectroscopy of the CH_2NC radical is important to obtain thermochemical properties (such as ionization energies or dissociative ionization thresholds) which are relevant for modeling its density and that of its cationic forms (CH_2NC^+ and its dissociative ionization fragments) in astrophysical media and VUV-irradiated complex media. In addition to the above-mentioned astrophysical context, these data can also provide a means of identification in gas-phase reaction experiments by their photoion efficiency curves or by their photoelectron spectroscopy. This is particularly true for nitriles and isonitriles as recently shown for CN, HNC and CNC.[15–17] The VUV photoionization spectroscopy of the isocyanomethyl radical, CH_2NC, has never been reported to our

[a] *Institut des Sciences Moléculaires d'Orsay, CNRS, Université Paris-Saclay, F-91405 Orsay (France).*
[b] *Synchrotron SOLEIL, L'Orme des Merisiers, Saint Aubin BP 48, F-91192 Gif sur Yvette Cedex, France*
[c] *Univ Rennes, Ecole Nationale Supérieure de Chimie de Rennes, CNRS, ISCR – UMR6226, F-35000 Rennes, France*
[d] *Institut des Sciences Moléculaires (ISM), CNRS, Univ. Bordeaux, 351 cours de la Libération, 33400, Talence, France*

† Electronic Supplementary Information (ESI) available: [TOF mass spectrum recoreded at 13.6 eV and, Ion yields and TPES of the species detected in our experiment and not presented in the paper]. See DOI: 10.1039/cXCP00000x/

* corresponding authors: berenger.gans@universite-paris-saclay.fr and jean-christophe.loison@u-bordeaux.fr

Accepted manuscript

knowledge, except for the calculated photoelectron spectrum of Horn *et al.*[18] In the present work, we present a first-time measurement of the mass-selected threshold photoelectron spectrum (TPES) of this radical and its vibrational assignment obtained by comparison with *ab initio* calculations.

2 Methodologies

2.1 Experimental

To generate the CH_2NC radical, we used a flow-tube reactor inducing H-abstraction from the methyl isocyanide (CH_3NC) precursor by reaction with F atoms. This reactor is located inside the permanent molecular beam end-station SAPHIRS of the DESIRS beamline at the SOLEIL synchrotron. This radical source and the DELICIOUS 3 spectrometer of SAPHIRS have been described in detail elsewhere.[19,20]

CH_3NC was synthesized following a slightly different procedure than the one described by Schuster *et al.*[21] p-Toluenesulfonyl chloride (38.1 g, 200 mmol, $m/z = 190.6$ a.m.u.), trioctylamine (70.7 g, 200 mmol, $m/z = 353.7$ a.m.u.), and then N-methylformamide (5.9 g, 100 mmol, $m/z = 59$ a.m.u.) were introduced into a 250 mL single-necked round-bottomed flask equipped with a stirring bar. The flask was fitted to a vacuum line equipped with two U-tubes with stopcocks. The pressure was stabilized at 2 mbar and the first U-tube was immersed in a liquid nitrogen bath. The mixture was allowed to warm up to 80°C over about 1 h. Methyl isocyanide was thus evacuated from the reaction mixture as it was formed and condensed in the trap. At the end of the reaction, the trap was allowed to warm up to room temperature, and the pure compound was condensed in the second trap cooled down to −100°C. This procedure led to 3.3 g of CH_3NC, (*i.e.* a yield of 80%). The methyl cyanide singlet (δ 2.01 ppm) was not detected in the ^{1}H NMR spectrum ($CDCl_3$, 400 MHz) of methyl isocyanide, which gives a maximum CH_3CN / CH_3NC ratio of 0.5%. The methyl isocyanide, a colorless bad-smelling liquid, can be kept under liquid nitrogen or under vacuum in the freezer for months.

The fluorine atoms were produced from a mixture of diluted F_2 (5% in He) dissociated in a microwave discharge and fed into the main reactor, while the CH_3NC precursor was introduced into a bubbler and carried into the quartz reactor injector using a flow of 100 sccm (standard cubic centimeters per minute) of He. The total pressure in the reactor was around 1 mbar for a total flow of 1200 sccm and the concentrations of F and CH_3NC were estimated to be around 1.0×10^{13} atoms·cm^{-3} and 2.0×10^{14} molecules·cm^{-3}, respectively. The CH_2NC radicals were then produced ($\approx 10^{13}$ molecules·cm^{-3}) releasing HF as a side product through the $CH_3NC + F \rightarrow CH_2NC + HF$ reaction. The mixing time between F and CH_3NC could be adjusted *via* the distance between the injector and a first skimmer, which is computer-controlled and was set in this study to approximately 1 ms. The resulting gas mixture was skimmed twice and reached the center of the ionization chamber, where the species were ionized by the tunable VUV synchrotron radiation from the undulator-based DESIRS beamline[22] at the French national synchrotron facility SOLEIL. The beamline was set to provide monochromatized and linearly polarized light with an estimated photon flux of 10^{13} ph·s^{-1} and a spectral resolution of 6 meV at 10 eV. A gas filter upstream of the monochromator was filled with krypton to effectively cut off the harmonics from the undulator spectrum and ensure a high spectral purity. A photodiode (AXUV, IRD) was used to measure the photon flux and to correct its energy-dependent fluctuations. The photon energy has been calibrated in the explored range with the ionization energies of methyl[23] and methylene[24] radicals to a precision of 3 meV. The electrons and ions formed at the center of the DELICIOUS 3 spectrometer were accelerated in opposite directions by a DC electric field of 88 V.cm^{-1}, and detected in coincidence by a velocity map imaging (VMI) and imaging linear time-of-flight (TOF) analyzers, respectively. Note that this electric field lowers the ionization energy by 7 meV,[25] and that all the final values given below have been shifted up accordingly. The double imaging photoelectron-photoion coincidence, i^{2}PEPICO, allows the spectroscopy study of the cation by scanning the photon energy in the $9.3 - 11.2$ eV range with 5 meV steps, and detecting the threshold photoelectron signal using a method described in section 3.3. The total (electron + photon) energy resolution was in this case 17 meV. In this work, the photon energy range was chosen to observe the origin band of the lowest photoionizing transition of CH_2NC while keeping the photon energy below the ionization energy (IE) of the precursor ($IE(CH_3NC) = 11.24$ eV).[26] The ion-kinetic-energy imaging was used to select only ions that possess a velocity component along the molecular beam direction, and provided an estimate of the translational temperature of the radicals ($T_{trans} \approx 150$ K).

2.2 Computational

The identification of the geometries of the ground and excited states of neutral and ionic species has been performed with the complete active space self-consistent field (CASSCF) method. The calculations were carried out using the MOLPRO 2012 package[27] and the Dunning augmented triple zeta cc-pVTZ basis.[28] The Franck-Condon (FC) factors for the photoionization of CH_2NC and CH_2CN were calculated using the harmonic approximation for the vibrational normal modes of the neutral and cationic ground states and the Condon approximation for the dipole moment. The Duschinsky effect was considered using recursive formulae already implemented in the Gaussian16 software package.[11] For FC calculations, the electronic structure calculations for geometry optimization and harmonic frequencies calculations were carried out at DFT level (M06-2X) using AVTZ basis set with Gaussian16. The vertical ionization of CH_2NC was also calculated using Gaussian software and Electron Propagator Theory with OVGF calculations and AVTZ basis set on optimized geometries calculated at the M06-2X/AVTZ level.

3 Results and discussions

3.1 Composition of the gas phase in the reactor

The gas phase composition of the reactor can be described using the mass spectra recorded at each photon energy of the 9.3 to 11.2 eV explored range. Fig. 1 shows the integrated result, *i.e.*,

Accepted manuscript

the sum of all the mass spectra in this energy range.

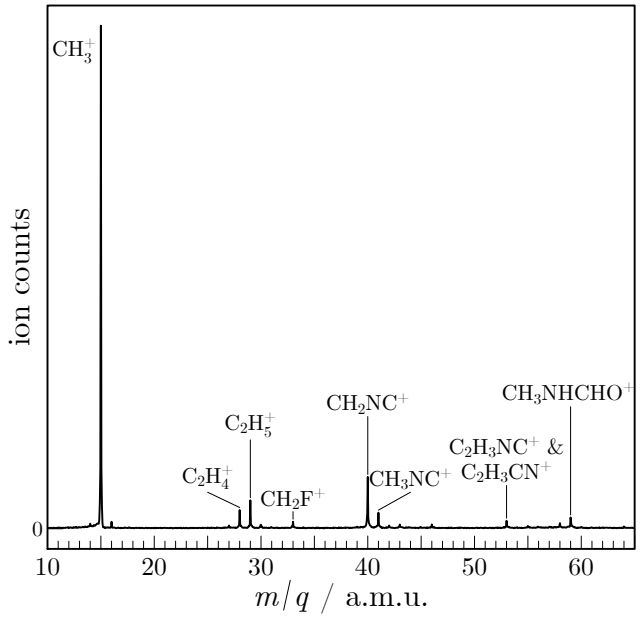


Fig. 1 TOF mass spectrum integrated between 9.3 and 11.2 eV photon energy showing the gas-phase composition of the reactor.

The reaction used in this experiment to produce the CH_2NC radical can lead to two reactive channels:

$$CH_3NC + F \rightarrow CH_2NC + HF \quad (\Delta_r H^{298} = -169 \text{ kJ/mol}) \quad (1)$$

$$CH_3NC + F \rightarrow CH_3 + FCN \quad (\Delta_r H^{298} = -94 \text{ kJ/mol}) \quad (2)$$

These two reactions occur in our reactor as confirmed by the two most intense peaks of Fig. 1 corresponding to the CH_3^+ ($m/q = 15$ a.m.u.) and CH_2NC^+ ($m/q = 40$ a.m.u.) radical cations. A Time-Of-Flight (TOF) mass spectrum recorded at 13.6 eV (see Fig. 1 of ESI) confirms the production of FCN strenghtening that the CH_3 radical is produced through the channel 2 of the CH_3NC + F reaction. Many other species are detected. Their number and diverse natures highlight the occurrence of a complex chemistry and the presence of impurities in our reactor which is overcome by the use of the PEPICO technique (*i.e.* the mass selectivity). Although not important for the following discussion, we are able to assign all of them using their photoelectron spectra and their ion yields (see Fig. 2 of ESI). Below the mass of the precursor ($m/q = 41$ a.m.u.), we also observed (see Fig. 1) CH_2 ($m/q = 14$ a.m.u.), $^{13}CH_3$ ($m/q = 16$ a.m.u.), C_2H_3 ($m/q = 27$ a.m.u.), C_2H_4 ($m/q = 28$ a.m.u.), C_2H_5 ($m/q = 29$ a.m.u.), H_2CO ($m/q = 30$ a.m.u.), CH_2F ($m/q = 33$ a.m.u.). The signal observed at the mass of the CH_3NC precursor ($m/q = 41$ a.m.u.) includes a weak contribution from the $^{13}CH_2NC^+$ (^{13}C natural isotope of CH_2NC^+) but mainly comes from the ionization of the precursor (CH_3NC^+ signal). Note that the explored energy range is below the *IE* of the precursor ($IE(CH_3NC) = 11.263(5)$ eV)[29] and thus the relatively weak signal which appears above 11 eV is likely due to excited vibrational levels of CH_3NC which are populated in the reactor and thus generate hot bands (see the corresponding ion yield in Fig. 2 of ESI). Above that mass, $m/q = 58$ a.m.u. and $m/q = 43$ a.m.u. are clear signatures of the acetone molecule (ionization ($CH_3COCH_3^+$) and dissociative ionization (CH_3CO^+), respectively).

The species responsible for the signal at $m/q = 59$ a.m.u. has an *IE* below the lower limit of the scan (9.3 eV). We can thus exclude CH_2FNC and CH_2FCN for which the *IE*s are above the explored range ($IE_{adia}(CH_2FNC) = 11.71$ eV (calculated at M06-2X/AVTZ level) and $IE_{vert.}(CH_2FCN) = 12.67$ eV[30]). Part of this signal is probably a signature of CH_3NHCHO (one of the precursors used in the CH_3NC synthesis, see section 2.1) which has an *IE* of 9.79 eV.[31] The TPES exhibits indeed three structures at 9.80, 9.88, and 10.08 eV in agreement with the results of Brundle *et al.*.[31]

Finally, the signal at $m/q = 53$ a.m.u. is most likely due to C_2H_3CN isomers. Indeed, C_2H_3CN has an *IE* of 10.91 eV[32] which is consistent with the position of the strongest band in our spectrum (10.909 eV, $IE = 10.916 \pm 0.010$ eV after field-induced shift correction), the bands located around 11.077 eV corresponding to transitions towards excited vibrational states of $C_2H_3CN^+$. The identifications of the bands located at 10.183 eV and 10.438 eV, which seem to correspond to an origin band and its vibrational component, respectively, are more challenging. C_2H_3NC is expected to be a good candidate considering the abundant species present in the reactor (CH_2NC and CH_3) but recent experimental work by Chrostowska *et al.* leads to an *IE* of 10.75 eV.[33] It should be noted that Chrostowska *et al.* have calculated the *IE* around 10.55 eV and we have calculated the *IE* of C_2H_3NC at 10.32 eV at M06-2X/AVTZ level, both being relatively different from the experimental determination. Further experimental and theoretical works are needed to clarify this point.

Interestingly, although we used very similar experimental conditions than in our previous paper in which we employed the CH_3CN precursor,[34,35] the CH_3NC + F and CH_3CN + F reactions are notably different. Indeed, in addition to the obvious large difference in CH_3 production, double and triple H atom abstractions (production of HCNC and CNC) and the production of CF are not observed in the case of CH_3NC + F. These behaviours clearly highlight the difference of the nitrile and isonitrile chemistries. These differences are suspected to be the origins of the HCN/HNC ratio variation over the interstellar media,[36] and should be studied in further detail in the future.

3.2 Ionization matrices and TIY

The mass-selected photoelectron signal as a function of electron kinetic energy and photon energy for isocyanomethyl CH_2NC ($m/q = 40$) is displayed as a two-dimensional color map in Fig. 2. The data in this 2D matrix can be reduced in different ways. The sum of all lines (integration over all electron kinetic energies) as a function of the photon energy leads to the total ionization yield (TIY), depicted in white in Fig. 2. Rich structures, signature of autoionizing neutral Rydberg states of CH_2NC, are observed in this TIY. Their assignment falls outside the scope of this article and is thus not discussed here. Similar resonances were reported in the case of CH_2CN.[34,37]

Accepted manuscript

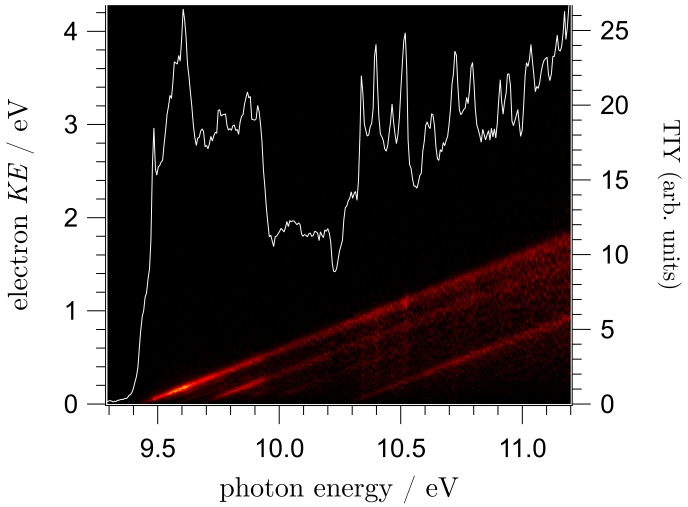


Fig. 2 Mass-selected photoelectron signal as a function of the photon energy (horizontal axis) and electron kinetic energy (vertical axis), for $m/q = 40$ a.m.u.. The corresponding total ion yield obtained by integrating over all electron kinetic energies is superimposed on the map as a white line.

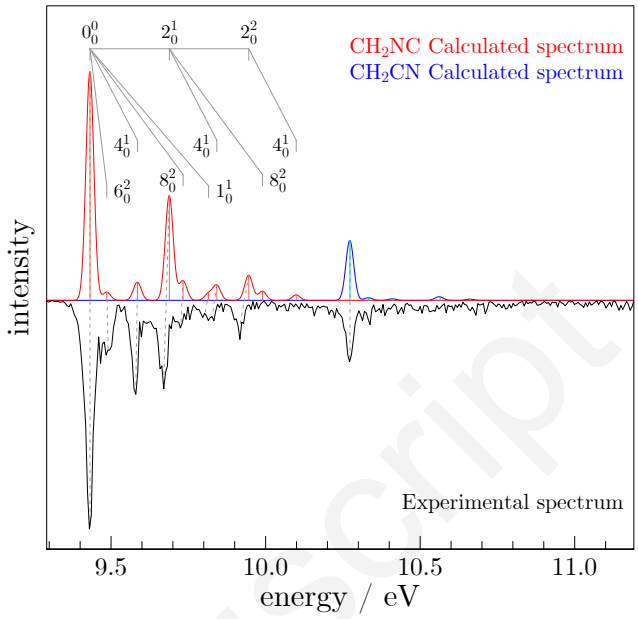


Fig. 3 Experimental TPES of $m/q = 40$ a.m.u. between 9.3 and 11.2 eV in black. The red and blue spectra correspond to our calculated photoelectron spectra of CH_2NC and CH_2CN, respectively, both shifted in energy to match the origin bands. Each calculation is displayed as a stick spectrum and as a convoluted stick spectrum (gaussian lineshape with $FWHM = 30$ meV) to account for the spectral resolution and the rotational contour of the bands. The grey dashed lines link the corresponding vibronic bands in the experimental and calculated spectra.

3.3 Threshold photoelectron spectra

From the 2D matrix displayed in Fig. 2, the threshold photoelectron spectrum can be obtained by integrating the photoelectron signal along diagonal lines of constant slope $KE = IE_i - h\nu$ corresponding to the i-th ionization energy:[38]

$$TPES(h\nu) = \int_0^{KE_{\max}} A(h\nu + KE, KE)\mathrm{d}E, \qquad (3)$$

where $A(h\nu, KE)$ is the 2D matrix in Fig. 2, and $KE_{\max}$ is the maximum kinetic energy used to generate the TPES, here 50 meV. The obtained spectrum with this method is often called a slow photoelectron spectrum (SPES). The result is similar to the better known threshold PES (TPES: sum of the matrix lines for only low kinetic energies of electrons),[39] but offers a better compromise between resolution and signal-to-noise ratio. For instance, in this case, an electron bandwidth of 50 meV leads to a 17 meV resolution. The TPES recorded for $m/q = 40$ a.m.u. is shown in Fig. 3 and corresponds to the $X^+\,^1A_1 \leftarrow X\,^2B_1$ ionizing transition of CH_2NC. It presents a strong adiabatic transition at 9.432 eV, followed by some vibrational structures. After the field-induced-shift correction, we deduce an adiabatic ionization energy of 9.439 ± 0.006 eV for the CH_2NC radical. This value is in very good agreement with our calculated value of 9.44 eV at M06-2X/AVTZ level. Nevertheless, this agreement should be nuanced considering the precision of our calculation method which is usually about 0.1 eV.

Our FC simulation is displayed in red in Fig. 3 and agrees well with our experimental spectrum and with the calculated spectrum of Horn *et al.*[18] The comparison between our calculated and experimental fundamental vibrational wavenumbers is reported in Table 1. Only the band located around 10.272 eV is not reproduced (see discussion below). From this simulation, we deduce that various vibrational modes are active upon ionization: the ν_6^+ (CNC out-of-plane bend), ν_4^+ (H_2C-NC stretch) , ν_2^+ (N-C stretch), ν_8^+ (CH_2 rock), and ν_1^+ (CH_2 symmetric stretch). The remaining band at 10.272 eV might be assigned to a photoionizing transition involving an excited electronic state of the cation. Nevertheless, our calculations predict that the transition involving the lowest excited electronic state of the cation should occur around 11.36 eV (calculated with the Electron Propagator Theory with Gaussian). Accordingly, no photoionizing transition involving a metastable state of the neutral species is predicted in this region. The first quadruplet state of CH_2NC ($a\,^4A_2$) is calculated 4.3 eV above the electronic ground state of CH_2NC and could ionize towards the first triplet state of CH_2NC^+ ($a^+\,^3B_1$). The corresponding adiabatic ionization energy is predicted at 6.9 eV. Although we started the measurement at 9.3 eV, this photoionizing transition should appear in the PES matrix (see Fig 2) as diagonal line above the diagonal of the $X^+\,^1A_1 \leftarrow X\,^2B_1$ transition (upper diagonal in the picture). The absence of such a signal indicates that the quadruplet state is not produced in the reactor. Moreover, the a $^4A_2$ metastable state of CH_2NC is not energetically accessible by the F + CH_3NC reaction ($\Delta_r H^\circ = 1.76$ eV). Nevertheless, although there is a noticeable cooling of the translational (and probably rotational) temperature due to the successive expansions through the two skimmers, the H abstraction reaction exothermicity (−169 kJ/mol) vibrationally excites the resulting CH_2NC radical (and, similarly, the HF molecule). Moreover, the transition state of the $CH_2NC \rightarrow CH_2CN$ isomerization reaction is located +121 kJ/mol above the CH_2NC ground state (at M06-

Accepted manuscript

Table 1 Calculated and experimental fundamental vibrational-mode wavenumbers ($\tilde{\nu}_i^+$) of the CH_2NC^+ cation. The vibrational mode labels correspond to the standard notation (sorted by lowering symmetries and decreasing wavenumbers).

Vibrational mode	Mode description	Symmetry	Calc. wavenumber (/ cm^{-1})	Exp. wavenumber (/ cm^{-1})
ν_1^+	CH_2 sym. stretch	a_1	3094.5	2999(80)
ν_2^+	N-C stretch	a_1	2071.4	1925(40)
ν_3^+	CH_2 scissor	a_1	1522.5	-
ν_4^+	H_2C-N stretch	a_1	1238.6	1193(40)
ν_5^+	CH_2 wag	b_1	1155.0	-
ν_6^+	CNC out-of-plane bend	b_1	218.9	237(50)[a]
ν_7^+	CH_2 asym. stretch	b_2	3217.9	-
ν_8^+	CH_2 rock	b_2	1214.4	1185(60)[b]
ν_9^+	CNC in-plane bend	b_2	252.8	-

[a] deduced from the 6_0^2 transition.
[b] deduced from the 8_0^2 transition.

2X/AVTZ level) in very good agreement with the value calculated by Moran *et al.* (+122 kJ/mol calculated at the MP4/6-311++G level).[12] Thus, one can suspect that some CH_2CN can be produced which can explain the band located at 10.272 eV in the TPES spectrum. The blue curve depicted in Fig. 3 corresponds to the FC simulation of the CH_2CN TPES[34,35] and matches perfectly the band at 10.272 eV. The corresponding *IE* is 10.279(6) eV after the correction of the field-induced shift, in good agreement with our previous work ($IE(CH_2CN = 10.275(3)$ eV)[34,35] and that of Steinbauer *et al.* ($IE(CH_2CN) = 10.28(2)$ eV).[40] Note that, the CH_2CN can also come from CH_3CN + F reaction if CH_3CN is somehow produced either in the reactor or during the CH_3NC synthesis.

4 Conclusions

We succeeded in efficiently producing the isocyanomethyl CH_2NC radical through the $CH_3NC + F \rightarrow CH_2NC + HF$ reaction in a flow-tube reactor. Ion yield and TPE spectra of this radical have been recorded for the first time employing the DELICIOUS 3 spectrometer of the DESIRS beamline of the SOLEIL synchrotron facility. We were able to assign the TPES using theoretical calculations (CASSCF and DFT methods) and thus to extract the adiabatic ionization energy of CH_2NC ($IE_{adia.} = 9.439(6)$ eV) and several fundamental vibrational wavenumbers of its cation. We have demonstrated the possibility of isonitrile radical production in large amounts (around 10^{13} molecules·cm^{-3}), which opens up new perspectives for the study of this radical, in connection to its importance in astrochemistry.

Conflicts of interest

There are no conflicts to declare.

Acknowledgements

This work was performed on the DESIRS beamline under proposal number 20181133. We acknowledge SOLEIL for provision of synchrotron radiation facilities and the DESIRS beamline staff for their assistance. This work received financial support from the French Agence Nationale de la Recherche (ANR) under grant ANR-12-BS08-0020-02 (project SYNCHROKIN). This work was supported by the Programme National Physique et Chimie du Milieu Interstellaire (PCMI) of CNRS/INSU with INC/INP co-funded by CEA and CNES. J.-C.G. thanks the CNES for a grant.

Notes and references

1 B. E. Turner, L. Pirogov and Y. C. Minh, *The Astrophysical Journal*, 1997, **483**, 235–261.
2 D. Bockelée-Morvan, N. Biver, E. Jehin, A. L. Cochran, H. Wiesemeyer, J. Manfroid, D. Hutsemékers, C. Arpigny, J. Boissier, W. Cochran, P. Colom, J. Crovisier, N. Milutinovic, R. Moreno, J. X. Prochaska, I. Ramirez, R. Schulz and J.-M. Zucconi, *The Astrophysical Journal Letters*, 2008, **679**, L49.
3 J. C. Loison, E. Hébrard, M. Dobrijevic, K. M. Hickson, F. Caralp, V. Hue, G. Gronoff, O. Venot and Y. Bénilan, *Icarus*, 2015, **247**, 218–247.
4 P. Gratier, J. Pety, V. Guzmán, M. Gerin, J. R. Goicoechea, E. Roueff and A. Faure, *Astronomy and Astrophysics*, 2013, **557**, A101.
5 H. Calcutt, M. R. Fiechter, E. R. Willis, H. S. P. Müller, R. T. Garrod, J. K. Jørgensen, S. F. Wampfler, T. L. Bourke, A. Coutens, M. N. Drozdovskaya, N. F. W. Ligterink and L. E. Kristensen, *Astronomy and Astrophysics*, 2018, **617**, A95.
6 K. Kawaguchi, M. Ohishi, S.-I. Ishikawa and N. Kaifu, *The Astrophysical Journal*, 1992, **386**, L51–L53.
7 I. Jiménez-Serra, I. Vasyunin Anton, P. Caselli, N. Marcelino, N. Billot, S. Viti, L. Testi, C. Vastel, B. Lefloch and R. Bachiller, *The Astrophysical Journal Letters*, 2016, **830**, L6.
8 M. Agúndez, J. Cernicharo, P. de Vicente, N. Marcelino, E. Roueff, A. Fuente, M. Gerin, M. Guélin, C. Albo, A. Barcia, L. Barbas, R. Bolaño, F. Colomer, M. C. Diez, J. D. Gallego, J. Gómez-González, I. López-Fernández, J. A. López-Fernández, J. A. López-Pérez, I. Malo, J. M. Serna and F. Tercero, *Astronomy and Astrophysics*, 2015, **579**, L10.
9 M. Agúndez, N. Marcelino and J. Cernicharo, *The Astrophysical Journal*, 2018, **861**, L22.
10 C. Vastel, J. C. Loison, V. Wakelam and B. Lefloch, *Astronomy and Astrophysics*, 2019, **625**, A91.

Accepted manuscript

11 M. J. Frisch, G. W. Trucks, H. B. Schlegel, G. E. Scuseria, M. A. Robb, J. R. Cheeseman, G. Scalmani, V. Barone, B. Mennucci, G. A. Petersson, H. Nakatsuji, M. Caricato, X. Li, H. P. Hratchian, A. F. Izmaylov, J. Bloino, G. Zheng, J. L. Sonnenberg, M. Hada, M. Ehara, K. Toyota, R. Fukuda, J. Hasegawa, M. Ishida, T. Nakajima, Y. Honda, O. Kitao, H. Nakai, T. Vreven, J. A. Montgomery Jr., J. E. Peralta, F. Ogliaro, M. Bearpark, J. J. Heyd, E. Brothers, K. N. Kudin, V. N. Staroverov, R. Kobayashi, J. Normand, K. Raghavachari, A. Rendell, J. C. Burant, S. S. Iyengar, J. Tomasi, M. Cossi, N. Rega, J. M. Millam, M. Klene, J. E. Knox, J. B. Cross, V. Bakken, C. Adamo, J. Jaramillo, R. Gomperts, R. E. Stratmann, O. Yazyev, A. J. Austin, R. Cammi, C. Pomelli, J. W. Ochterski, R. L. Martin, K. Morokuma, V. G. Zakrzewski, G. A. Voth, P. Salvador, J. J. Dannenberg, S. Dapprich, A. D. Daniels, Ö. Farkas, J. B. Foresman, J. V. Ortiz, J. Cioslowski and D. J. Fox, *Gaussian 16 Revision C.01*.

12 S. Moran, H. B. Ellis, D. J. DeFrees, A. D. McLean, S. E. Paulson and G. B. Ellison, *Journal of the American Chemical Society*, 1987, **109**, 6004–6010.

13 H. Sun, H.-Q. He, B. Hong, Y.-F. Chang, Z. An and R.-S. Wang, *International Journal of Quantum Chemistry*, 2006, **106**, 894–905.

14 W. Zhang and B. Du, *International Journal of Quantum Chemistry*, 2006, **106**, 1076–1085.

15 B. Gans, G. A. Garcia, S. Boyé-Péronne, S. T. Pratt, J.-C. Guillemin, A. Aguado, O. Roncero and J.-C. Loison, *Physical Chemistry Chemical Physics*, 2019, **21**, 2337–2344.

16 L. Coudert, B. Gans, G. Garcia and J.-C. Loison, *The Journal of Chemical Physics*, 2018, **148**, 054302.

17 B. Gans, S. Boyé-Péronne, G. Garcia, A. Röder, D. Schleier, P. Halvick and J.-C. Loison, *The Journal of Physical Chemistry Letters*, 2017, **8**, 4038–4042.

18 M. Horn, M. Oswald, R. Oswald and P. Botschwina, *Berichte der Bunsengesellschaft für physikalische Chemie*, 1995, **99**, 323–331.

19 G. A. Garcia, X. Tang, J.-F. Gil, L. Nahon, M. Ward, S. Batut, C. Fittschen, C. A. Taatjes, D. L. Osborn and J.-C. Loison, *The Journal of Chemical Physics*, 2015, **142**, 164201.

20 X. Tang, G. A. Garcia, J.-F. Gil and L. Nahon, *Review of Scientific Instruments*, 2015, **86**, 123108.

21 R. E. Schuster, J. E. Scott and A. Casanova Jr., *Organic Syntheses*, 1966, **46**, 75–77.

22 L. Nahon, N. de Oliveira, G. A. Garcia, J.-F. Gil, B. Pilette, O. Marcouillé, B. Lagarde and F. Polack, *Journal of Synchrotron Radiation*, 2012, **19**, 508–520.

23 A. M. Schulenburg, C. Alcaraz, G. Grassi and F. Merkt, *The Journal of Chemical Physics*, 2006, **125**, 104310.

24 S. Willitsch, L. L. Imbach and F. Merkt, *The Journal of Chemical Physics*, 2002, **117**, 1939–1940.

25 F. Merkt, A. Osterwalder, R. Seiler, R. Signorell, H. Palm, H. Schmutz and R. Gunzinger, *Journal of Physics B - Atomic Molecular and Optical Physics*, 1998, **31**, 1705–1724.

26 R. F. Lake and H. W. Thompson, *Spectrochimica Acta Part A: Molecular Spectroscopy*, 1971, **27**, 783–786.

27 H. Werner, P. J. Knowles, G. Knizia, F. R. Manby and M. Schütz, *Wiley Interdisciplinary Reviews: Computational Molecular Science*, 2012, **2**, 242–253.

28 T. H. Dunning Jr, *The Journal of Chemical Physics*, 1989, **90**, 1007–1023.

29 A. Bellili, Z. Gouid, M. C. Gazeau, Y. Bénilan, N. Fray, J. C. Guillemin, M. Hochlaf and M. Schwell, *Physical Chemistry Chemical Physics*, 2019, **21**, 26017–26026.

30 R. Botter, Y. Gounelle, Y. Henry, J. Jullien, F. Menes and D. Solgadi, *Journal of Electron Spectroscopy and Related Phenomena*, 1977, **10**, 393–405.

31 C. R. Brundle, D. W. Turner, M. B. Robin and H. Basch, *Chemical Physics Letters*, 1969, **3**, 292–296.

32 K. Ohno, S. Matsumoto, K. Imai and Y. Harada, *The Journal of Physical Chemistry*, 1984, **88**, 206–209.

33 A. Chrostowska, M. Abdellatif, M. Daisuke, S. Khayar, H. Ushiki, A. Graciaa, L. Belachemi and J.-C. Guillemin, *ChemPhysChem*, 2012, **13**, 226–236.

34 G. A. Garcia, J. Krüger, B. Gans, C. Falvo, L. H. Coudert and J.-C. Loison, *The Journal of Chemical Physics*, 2017, **147**, 13908.

35 G. A. Garcia, J. Krüger, B. Gans, C. Falvo, L. H. Coudert and J.-C. Loison, *The Journal of Chemical Physics*, 2020, **152**, 169903.

36 A. Hacar, A. D. Bosman and E. F. van Dishoeck, *Astronomy and Astrophysics*, 2020, **635**, A4.

37 R. P. Thorn Jr, P. S. Monks, L. J. Steif, S. C. Kuo, Z. Zhang, S. K. Ross and R. B. Klemm, *The Journal of Physical Chemistry A*, 1998, **102**, 846–851.

38 J. C. Poully, J. P. Schermann, N. Nieuwjaer, F. Lecomte, G. Gregoire, C. Desfrancois, G. A. Garcia, L. Nahon, D. Nandi, L. Poisson and M. Hochlaf, *Physical Chemistry Chemical Physics*, 2010, **12**, 3566–3572.

39 T. Baer and R. P. Tuckett, *Physical Chemistry Chemical Physics*, 2017, **19**, 9698–9723.

40 M. Steinbauer, P. Hemberger, I. Fischer, M. Johnson and A. Bodi, *Chemical Physics Letters*, 2010, **500**, 232–236.

Accepted manuscript